Westinghouse Energy Systems

WESTINGHOUSE PROPRIETARY CLASS 3

WCAP-12874

TECHNICAL JUSTIFICATION FOR ELIMINATING PRESSURIZER SURGE LINE RUPTURE AS THE STRUCTURAL DESIGN BASIS FOR KEWAUNEE NUCLEAR PLANT

June 1991

D. C. Bhowmick
S. A. Swamy Y. S. Lee
D. E. Prager K. R. Hsu

Verified: _____
J. C. Schmertz
Structural Mechanics Technology

Approved: _____
S. S. Palusamy, Manager
Diagnostics and Monitoring Technology

Work Performed Under Shop Order: KFBP-950

WESTINGHOUSE ELECTRIC CORPORATION
Nuclear and Advanced Technology Division
P.O. Box 2728
Pittsburgh, Pennsylvania 15230-2728

TABLE OF CONTENTS

TABLE OF CONTENTS (cont.)

LIST OF TABLES

LIST OF FIGURES

LIST OF FIGURES (cont.)

SECTION 1.0
INTRODUCTION

1.1 Background

The current structural design basis for the pressurizer surge line requires postulating non-mechanistic circumferential and longitudinal pipe breaks. This results in additional plant hardware (e.g. pipe whip restraints) which would mitigate the dynamic consequences of the pipe breaks. It is, therefore, highly desirable to be realistic in the postulation of pipe breaks for the surge line. Presented in this report are the descriptions of a mechanistic pipe break evaluation method and the analytical results that can be used for establishing that a circumferential type break will not occur within the pressurizer surge line. The evaluations considering circumferentially oriented flaws cover longitudinal cases. The pressurizer surge line is known to be subjected to thermal stratification and the effects of thermal stratification for Kewaunee surge line has been evaluated and documented in WCAP-12841. The results of the stratification evaluation as described in WCAP-12841 have been used in the leak-before-break evaluation presented in this report.

1.2 Scope and Objective

The general purpose of this investigation is to demonstrate leak-before-break for the pressurizer surge line. The scope of this work covers the entire pressurizer surge line from the primary loop nozzle junction to the pressurizer nozzle junction. A schematic drawing of the piping system is shown in Section 3.0. The recommendations and criteria proposed in NUREG 1061 Volume 3 (1-1) are used in this evaluation. The criteria and the resulting steps of the evaluation procedure can be briefly summarized as follows:

1) Calculate the applied loads. Identify the location at which the highest stress occurs.

2) Identify the materials and the associated material properties.

3) Postulate a surface flaw at the governing location. Determine fatigue crack growth. Show that a through-wall crack will not result.

4) Postulate a through-wall flaw at the governing location. The size of the flaw should be large enough so that the leakage is assured of detection with margin using the installed leak detection equipment when the pipe is subjected to normal operating loads. A margin of 10 is demonstrated between the calculated leak rate and the leak detection capability.

5) Using maximum faulted loads, demonstrate that there is a margin of at least 2 between the leakage size flaw and the critical size flaw.

6) Review the operating history to ascertain that operating experience has indicated no particular susceptibility to failure from the effects of corrosion, water hammer or low and high cycle fatigue.

7) For the materials actually in the plant provide the material properties and justify that the properties used in the evaluation are representative of the plant specific material.

The flaw stability analyses is performed using the methodology described in SRP 3.6.3 (Reference 1-2).

The leak rate is calculated for the normal operating condition. The leak rate prediction model used in this evaluation is an [----------
----
--.----------]^{a,c,e} The crack opening area required for calculating the leak rates is obtained by subjecting the postulated through-wall flaw to normal operating loads (Reference 1-3). Surface roughness is accounted for in determining the leak rate through the postulated flaw.

The computer codes used in this evaluation for leak rate and fracture mechanics calculations have been validated (bench marked).

1.3 References

1-1 Report of the U.S. Nuclear Regulatory Commission Piping Review Committee - Evaluation of Potential for Pipe Breaks, NUREG 1061, Volume 3, November 1984.

1-2 Standard Review Plan; public comments solicited; 3.6.3 Leak-Before-Break Evaluation Procedures; Federal Register/Vol. 52, No. 167/Friday, August 28, 1987/Notices, pp. 32626-32633.

1-3 NUREG/CR-3464, 1983, "The Application of Fracture Proof Design Methods Using Tearing Instability Theory to Nuclear Piping Postulated Circumferential Through Wall Cracks."

1-4 WCAP 12841, Structural Evaluation of the Kewaunee Pressurizer Surge Line, Considering the Effects of Thermal Stratification

SECTION 2.0

OPERATION AND STABILITY OF THE PRESSURIZER SURGE LINE AND THE REACTOR COOLANT SYSTEM

2.1 Stress Corrosion Cracking

The Westinghouse reactor coolant system primary loop and connecting Class 1 lines have an operating history that demonstrates the inherent operating stability characteristics of the design. This includes a low susceptibility to cracking failure from the effects of corrosion (e.g., intergranular stress corrosion cracking). This operating history totals over 400 reactor-years, including five plants each having over 15 years of operation and 15 other plants each with over 10 years of operation.

In 1978, the United States Nuclear Regulatory Commission (USNRC) formed the second Pipe Crack Study Group. (The first Pipe Crack Study Group established in 1975 addressed cracking in boiling water reactors only.) One of the objectives of the second Pipe Crack Study Group (PCSG) was to include a review of the potential for stress corrosion cracking in Pressurized Water Reactors (PWR's). The results of the study performed by the PCSG were presented in NUREG-0531 (Reference 2-1) entitled "Investigation and Evaluation of Stress Corrosion Cracking in Piping of Light Water Reactor Plants." In that report the PCSG stated:

> "The PCSG has determined that the potential for stress-corrosion cracking in PWR primary system piping is extremely low because the ingredients that produce IGSCC are not all present. The use of hydrazine additives and a hydrogen overpressure limit the oxygen in the coolant to very low levels. Other impurities that might cause stress-corrosion cracking, such as halides or caustic, are also rigidly controlled. Only for brief periods during reactor shutdown when the coolant is exposed to the air and during the subsequent startup are conditions even marginally capable of producing stress-corrosion cracking in the primary systems of PWRs.

Operating experience in PWRs supports this determination. To date, no stress-corrosion cracking has been reported in the primary piping or safe ends of any PWR."

During 1979, several instances of cracking in PWR feedwater piping led to the establishment of the third PCSG. The investigations of the PCSG reported in NUREG-0691 (Reference 2-2) further confirmed that no occurrences of IGSCC have been reported for PWR primary coolant systems.

As stated above, for the Westinghouse plants there is no history of cracking failure in the reactor coolant system loop or pressurizer surge line piping. The discussion below further qualifies the PCSG's findings.

For stress corrosion cracking (SCC) to occur in piping, the following three conditions must exist simultaneously: high tensile stresses, susceptible material, and a corrosive environment. Since some residual stresses and some degree of material susceptibility exist in any stainless steel piping, the potential for stress corrosion is minimized by properly selecting a material immune to SCC as well as preventing the occurrence of a corrosive environment. The material specifications consider compatibility with the system's operating environment (both internal and external) as well as other material in the system, applicable ASME Code rules, fracture toughness, welding, fabrication, and processing.

The elements of a water environment known to increase the susceptibility of austenitic stainless steel to stress corrosion are: oxygen, fluorides, chlorides, hydroxides, hydrogen peroxide, and reduced forms of sulfur (e.g., sulfides, sulfides, and thionates). Strict pipe cleaning standards prior to operation and careful control of water chemistry during plant operation are used to prevent the occurrence of a corrosive environment. Prior to being put into service, the piping is cleaned internally and externally. During flushes and preoperational testing, water chemistry is controlled in accordance with written specifications. Requirements on chlorides, fluorides, conductivity, and pH are included in the acceptance criteria for the piping.

During plant operation, the reactor coolant water chemistry is monitored and maintained within very specific limits. Contaminant concentrations are kept below the thresholds known to be conducive to stress corrosion cracking with the major water chemistry control standards being included in the plant operating procedures as a condition for plant operation. For example, during normal power operation, oxygen concentration in the RCS and connecting Class 1 lines is expected to be in the ppb range by controlling charging flow chemistry and maintaining hydrogen in the reactor coolant at specified concentrations. Halogen concentrations are also stringently controlled by maintaining concentrations of chlorides and fluorides within the specified limits. This is assured by controlling charging flow chemistry. Thus during plant operation, the likelihood of stress corrosion cracking is minimized.

2.2 Water Hammer

Overall, there is a low potential for water hammer in the RCS and connecting surge lines since they are designed and operated to preclude the voiding condition in normally filled lines. The RCS and connecting surge line including piping and components, are designed for normal, upset, emergency, and faulted condition transients. The design requirements are conservative relative to both the number of transients and their severity. Relief valve actuation and the associated hydraulic transients following valve opening are considered in the system design. Other valve and pump actuations are relatively slow transients with no significant effect on the system dynamic loads. To ensure dynamic system stability, reactor coolant parameters are stringently controlled. Temperature during normal operation is maintained within a narrow range by control rod position; pressure is controlled by pressurizer heaters and pressurizer spray also within a narrow range for steady-state conditions. The flow characteristics of the system remain constant during a fuel cycle because the only governing parameters, namely system resistance and the reactor coolant pump characteristics are controlled in the design process. Additionally, Westinghouse has instrumented typical reactor coolant systems to verify the flow and vibration characteristics of the system and connecting surge lines. Preoperational testing and operating experience have verified the Westinghouse approach. The operating transients

of the RCS primary piping and connected surge lines are such that no significant water hammer can occur.

2.3 Low Cycle and High Cycle Fatigue

Low cycle fatigue considerations are accounted for in the design of the piping system through the fatigue usage factor evaluation to show compliance with the rules of Section III of the ASME Code. A further evaluation of the low cycle fatigue loading is discussed in Section 6.0 as part of this study in the form of a fatigue crack growth analysis.

Pump vibrations during operation would result in high cycle fatigue loads in the piping system. During operation, an alarm signals the exceedance of the RC pump shaft vibration limits. Field measurements have been made on the reactor coolant loop piping of a number of plants during hot functional testing. Stresses in the elbow below the RC pump have been found to be very small, between 2 and 3 ksi at the highest. Recent field measurements on typical PWR plants indicate vibration amplitudes less than 1 ksi. When translated to the connecting surge line, these stresses would be even lower, well below the fatigue endurance limit for the surge line material and would result in an applied stress intensity factor below the threshold for fatigue crack growth.

2.4 Summary Evaluation of Surge Line for Potential Degradation During Service

There has never been any service cracking or wall thinning identified in the pressurizer surge lines of Westinghouse PWR design. Sources of such degradation are mitigated by the design, construction, inspection, and operation of the pressurizer surge piping.

There is no mechanism for water hammer in the pressurizer/surge system. The pressurizer safety and relief piping system which is connected to the top of the pressurizer could have loading from water hammer events. However, these loads are effectively mitigated by the pressurizer and have a negligible effect on the surge line.

Wall thinning by erosion and erosion-corrosion effects will not occur in the surge line due to the low velocity, typically less than 1.0 ft/sec and the material, austenitic stainless steel, which is highly resistant to these degradation mechanisms. Per NUREG-0691, a study of pipe cracking in PWR piping, only two incidents of wall thinning in stainless steel pipe were reported and these were not in the surge line. Although it is not clear from the report, the cause of the wall thinning was related to the high water velocity and is therefore clearly not a mechanism which would affect the surge line.

It is well known that the pressurizer surge lines are subjected to thermal stratification and the effects of stratification are particularly significant during certain modes of heatup and cooldown operation. The effects of stratification have been evaluated for the Kewaunee surge line and the loads, accounting for the stratification effects, have been derived in WCAP-12841. These loads are used in the leak-before-break evaluation described in this report.

The Kewaunee Nuclear Plant surge line piping and associated fittings are forged product forms (see Section 3) which are not susceptible to toughness degradation due to thermal aging.

Finally, the maximum operating temperature of the pressurizer surge piping, which is about 650°F, is well below the temperature which would cause any creep damage in stainless steel piping.

2.5 References

2-1 Investigation and Evaluation of Stress-Corrosion Cracking in Piping of Light Water Reactor Plants, NUREG-0531, U.S. Nuclear Regulatory Commission, February 1979.

2-2 Investigation and Evaluation of Cracking Incidents in Piping in Pressurized Water Reactors, NUREG-0691, U.S. Nuclear Regulatory Commission, September 1980.

SECTION 3.0
MATERIAL CHARACTERIZATION

3.1 Pipe and Weld Materials

The pipe material of the pressurizer surge line for the Kewaunee Nuclear Plant are A376/TP316 and A403/WP316. These are a wrought product form of the type used for the primary loop piping of several PWR plants. The surge line is connected to the primary loop nozzle at one end and the other end of the surge line is connected to the pressurizer nozzle. The surge line system does not include any cast pipe or cast fitting. The welding processes used are shielded metal arc (SMAW) and submerged arc (SAW). Weld locations are identified in Figure 3-1.

In the following section the tensile properties of the materials are presented for use in the leak-before-break analyses.

3.2 Material Properties

The room temperature mechanical properties of the Kewaunee Nuclear Plant surge line materials were obtained from the Certified Materials Test Reports and are given in Table 3-1. The room temperature ASME Code minimum properties are given in Table 3-2. It is seen that the measured properties well exceed those of the Code. The representative minimum and average tensile properties were established (see Table 3-3). The material properties at temperatures (135°F, 205°F, 455°F, and 653°F) are required for the leak rate and stability analyses discussed later. The minimum and average tensile properties were calculated by using the ratio of the ASME Code Section III properties at the temperatures of interest stated above. Table 3-2 shows the tensile properties at various temperatures. The modulus of elasticity values were established at various temperatures from the ASME Code Section III (Table 3-4). In the leak-before-break evaluation, the representative minimum properties at temperature are used for the flaw stability evaluations and the representative

average properties are used for the leak rate predictions. The minimum ultimate stresses are used for stability analyses. These properties are summarized in Table 3-3.

3.3 References

3-1 ASME Boiler and Pressure Vessel Code Section III, Division 1, Appendices July 1, 1989.

TABLE 3-1

Room Temperature Mechanical Properties of the Pressurizer Surge Line Materials and Welds

ID	HEAT NO./SERIAL NO.	MATERIAL	YIELD STRENGTH (psi)	ULTIMATE STRENGTH (psi)	ELONG. (%)	R/A (%)
1	J2338/6302	A376/TP316	41,800	84,900	44.4	52.5
			43,700	90,400	48.1	67.9
2	J2338/6303	A376/TP316	41,600	86,900	46.6	68.9
			44,300	86,400	49.1	69.7
3	J2338/6303	A376/TP316	41,600	86,900	46.6	68.9
			44,300	86,400	49.1	69.7
4	J2009/5794	A376/TP316	41,900	86,400	51.8	65.9
			57,300	81,400	57.4	71.4
5	J2471/1048	A403/WP316	41,600	84,400	51.2	70.2

Shop Weld (SW) - Fabricated by SAW (worst case selected for conservatism)

Field Weld (FW) - Fabricated by GTAW/SMAW combination

TABLE 3-2

Room Temperature ASME Code Minimum Properties

Material	Yield Stress (psi)	Ultimate Stress (psi)
A376/TP316	30,000	75,000
A403/WP316	30,000	75,000

TABLE 3-3

Representative Tensile Properties for Kewaunee

Material	Temperature (°F)	Minimum Yield (psi)	Average Yield (psi)	Minimum Ultimate (psi)
A376/TP316	135	39,560	42,370	81,400
	205	35,610	38,140	81,300
	455	28,520	30,550	77,920
	653	25,630	27,490	77,920
A403/WP316	135	39,560	39,560	84,400
	205	35,610	35,610	84,310
	455	28,520	28,520	80,790
	653	25,630	25,630	80,790

TABLE 3-4

Modulus of Elasticity (E)

Temperature (°F)	E (ksi)
135	27,950
205	27,600
455	26,115
653	25,035

FW: FIELD WELD
SW: SHOP WELD

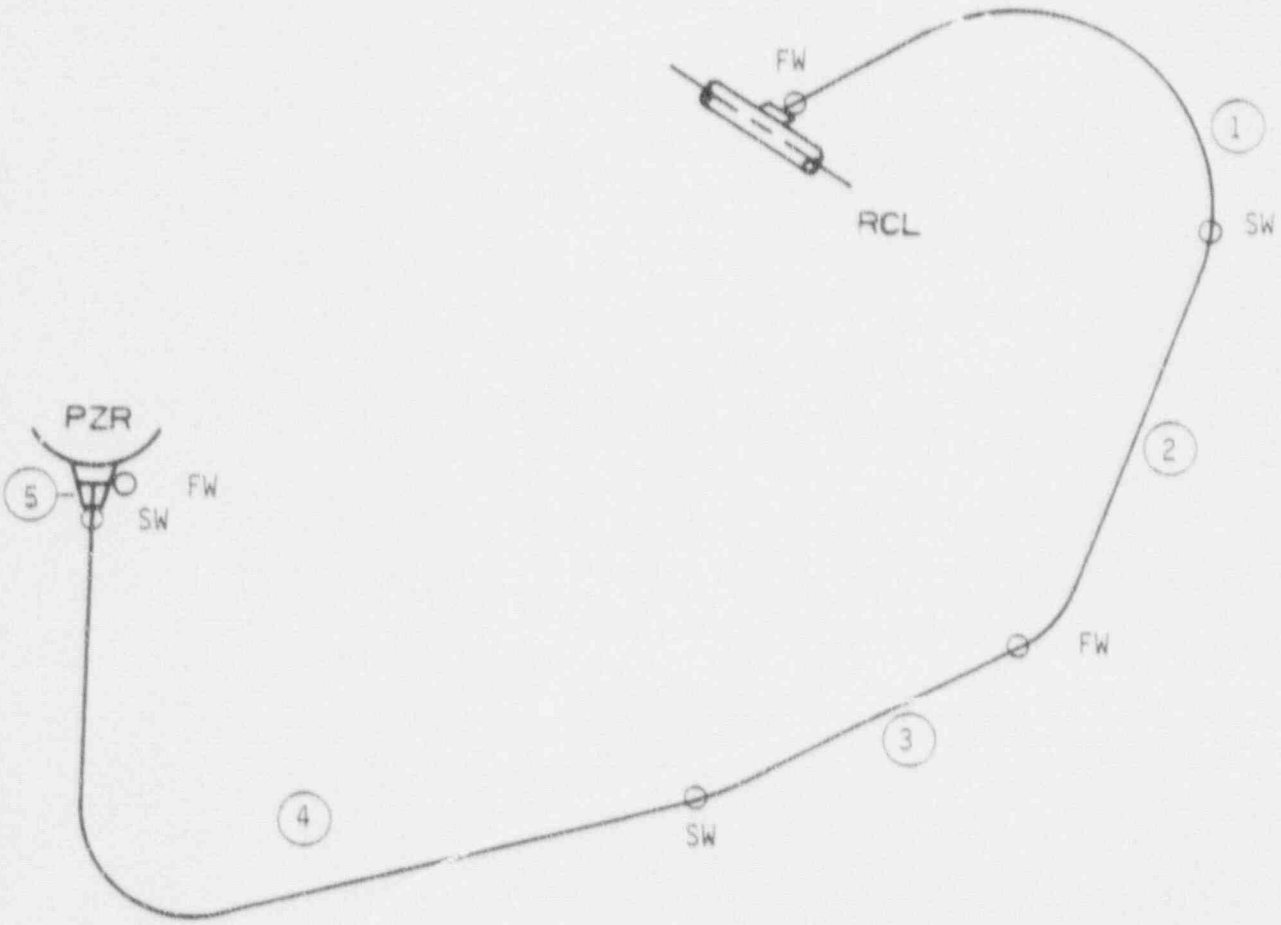

Figure 3-1 Kewaunee Surge Line Layout

SECTION 4.0

LOADS FOR FRACTURE MECHANICS ANALYSIS

Figures 3-1 shows schematic layout of the surge line for Kewaunee and identify the weld locations.

The stresses due to axial loads and bending moments were calculated by the following equation:

$$\sigma = \frac{F}{A} + \frac{M}{Z} \qquad (4\text{-}1)$$

where,

σ	=	stress
F	=	axial load
M	=	bending moment
A	=	metal cross-sectional area
Z	=	section modulus

The bending moments for the desired loading combinations were calculated by the following equation:

$$M_B = (M_Y^2 + M_Z^2)^{0.5} \qquad (4\text{-}2)$$

where,

M_B	=	bending moment for required loading
M_Y	=	Y component of bending moment
M_Z	=	Z component of bending moment

The axial load and bending moments for crack stability analysis and leak rate predictions are computed by the methods to be explained in Sections 4.1 and 4.2 which follow.

4.1 Loads for Crack Stability Analysis

The faulted loads for the crack stability analysis were calculated by the absolute sum method as follows:

$$F = |F_{DW}| + |F_{TH}| + |F_p| + |F_{SSE}| \quad (4\text{-}3)$$

$$M_Y = |M_{YDW}| + |M_{Y\ TH}| + |M_{Y\ SSE}| \quad (4\text{-}4)$$

$$M_Z = |M_{ZDW}| + |M_{Z\ TH}| + |M_{Z\ SSE}| \quad (4\text{-}5)$$

DW = Deadweight
TH = Applicable thermal load (normal or stratified)
P = Load due to internal pressure
SSE = SSE loading including seismic anchor motion

4.2 Loads for Leak Rate Evaluation

The normal operating loads for leak rate predictions were calculated by the algebraic sum method as follows:

$$F = F_{DW} + F_{TH} + F_p \quad (4\text{-}6)$$

$$M_Y = (M_Y)_{DW} + (M_Y)_{TH} \quad (4\text{-}7)$$

$$M_Z = (M_Z)_{DW} + (M_Z)_{TH} \quad (4\text{-}8)$$

The parameters and subscripts are the same as those explained in Section 4.1.

4.3 Loading Conditions

Because thermal stratification can cause large stresses at heatup and cooldown temperatures in the range of 455°F, a review of stresses was used to identify the worst situations for LBB applications. The loading states so identified are given in Table 4-1.

Seven loading cases were identified for LBB evaluation as given in Table 4-2. Cases A, B, C are cases for leak rate calculations with the remaining cases being the corresponding faulted situations for stability evaluations.

The cases postulated for leak-before-break are summarized in Table 4-3. The cases of primary interest are the postulation of a detectable leak at normal power conditions [----------]^{a,c,e}

The combination [----------]^{a,c,e}

The more realistic cases [----------
---------- ----------

----------]^{a,c,e}

[----------

----------]^{a,c,e} The logic for this ΔT [-------]^{a,c,e} is based on the following:

Actual practice, based on experience of other plants with this type of situation, indicates that the plant operators complete the cooldown as quickly as possible once a leak in the primary system is detected. Technical Specifications require cold shutdown within 24 hours but actual practice is that the plant depressurizes the system as soon as possible once a primary system leak is detected. Therefore, the hot leg is generally on the warmer side of the limits ()200°F) when the pressurizer bubble is quenched. Once the bubble is quenched, the pressurizer is cooled down fairly quickly reducing the ΔT in the system.

4.4 Summary of Loads and Geometry

The load combinations were evaluated at the various weld locations. Normal loads were determined using the algebraic sum method whereas faulted loads were combined using the absolute sum method.

4.5 Governing Locations

All the welds at Kewaunee surgeline are fabricated using the SMAW and SAW procedure. The following governing locations were established for the welds. Figure 4-1 shows the governing locations.

SMAW Weld

Node 1020.

SAW Weld

Node 1240.

The loads and stresses at these governing locations for all the loading combinations are shown in Tables 4-4.

TABLE 4-1

Types of Loadings

Pressure (P)

Dead Weight (DW)

Normal Operating Thermal Expansion (TH)

Safe Shutdown Earthquake and Seismic Anchor Motion (SSE)[a]

[a,c,e

]

[a]SSE is used to refer to the absolute sum of these loadings.

TABLE 4-2

Normal and Faulted Loading Cases for Leak-Before-Break Evaluations

CASE A: This is the normal operating case at 653°F consisting of the algebraic sum of the loading components due to P, DW and TH.

CASE B: [a,c,e

CASE C:]

CASE D: This is the faulted operating case at 653°F consisting of the absolute sum (every component load is taken as positive) of P, DW, TH and SSE.

CASE E: [a,c,e

CASE F:

CASE G:]

TABLE 4-3

Associated Load Cases for Analyses

A/D This is here-to-fore standard leak-before-break evaluation.

a,c,e

A/F

B/E

B/F

B/G[a]

C/G[a]

---

[a] These are judged to be low probability events.

TABLE 4-4

Summary of LBB Loads and Stresses by Case for Governing Locations

Node	Case	F_X(lbs)	S_X(psi)	M_B(in-lb)	S_B(psi)	S_T(psi)	
1020	A	134150	4943	835533	13468	18411	
1020	-	------	----	-------	-----	-----	a,c,e
1020	-	-----	---	-------	-----	-----	
1020	D	151864	5596	1150890	18551	24146	
1020	-	------	----	-------	-----	-----	a,c,e
1020	-	-----	----	------	-----	-----	
1020	-	-----	----	-------	-----	-----	
1240	A	140976	5194	564140	9093	14287	
1240	-	------	----	------	----	-----	a,c,e
1240	-	-----	----	-------	-----	-----	
1240	D	149846	5521	1169853	18856	24377	
1240	-	------	----	-------	-----	-----	a,c,e
1240	-	-----	----	------	-----	-----	
1240		-----	----	-------	-----	-----	

- o PIPE 10" SCHEDULE 140
- o MINIMUM WALL THICKNESS 0.875"

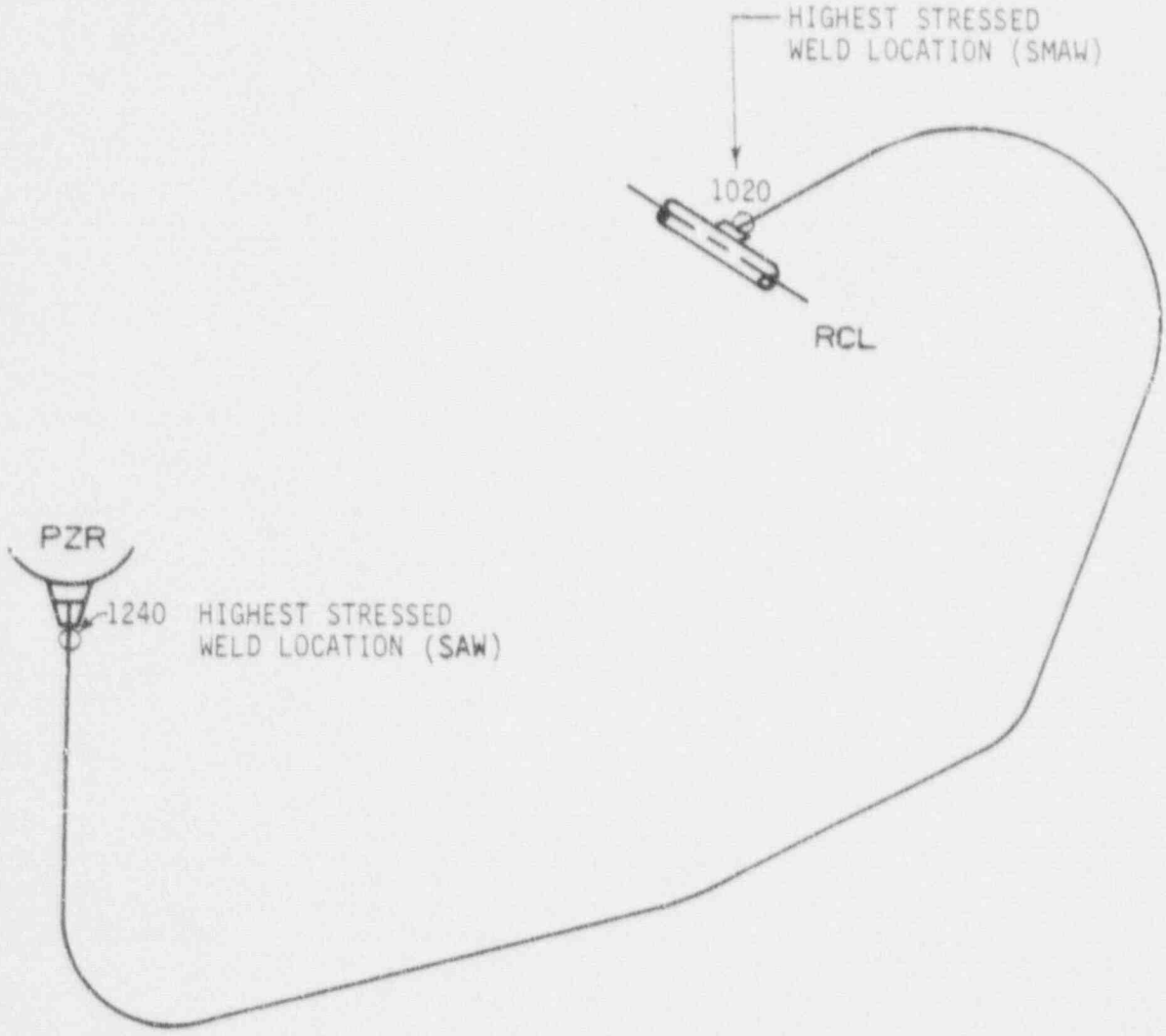

Figure 4-1 Kewaunee Surge Line Showing Governing Locations

SECTION 5.0
FRACTURE MECHANICS EVALUATION

5.1 Global Failure Mechanism

Determination of the conditions which lead to failure in stainless steel should be done with plastic fracture methodology because of the large amount of deformation accompanying fracture. One method for predicting the failure of ductile material is the [----------]^{a,c,e} method, based on traditional plastic limit load concepts, but accounting for [----------]^{a,c,e} and taking into account the presence of a flaw. The flawed component is predicted to fail when the remaining net section reaches a stress level at which a plastic hinge is formed. The stress level at which this occurs is termed as the flow stress. [----------
----------]^{a,c,e} This methodology has been shown to be applicable to ductile piping through a large number of experiments and is used here to predict the critical flaw size in the pressurizer surge line. The failure criterion has been obtained by requiring equilibrium of the section containing the flaw (Figure 5-1) when loads are applied. The detailed development is provided in Appendix A for a through-wall circumferential flaw in a pipe section with internal pressure, axial force, and imposed bending moments. The limit moment for such a pipe is given by:

[---]^{a,c,e} (5-1)

where:

[----------
---- ----------
------ ----------
---- ----------]^{a,c,e}

[

]^{a,c,e} (5-2)

The analytical model described above accurately accounts for the internal pressure as well as imposed axial force as they affect the limit moment. Good agreement was found between the analytical predictions and the experimental results (reference 5-1). Flaw stability evaluations, using this analytical model, are presented in section 5.3.

5.2 Leak Rate Predictions

Fracture mechanics analysis shows in general that postulated through-wall cracks in the surge line would remain stable and do not cause a gross failure of this component. However, if such a through-wall crack did exist, it would be desirable to detect the leakage such that the plant could be brought to a safe shutdown condition. The purpose of this section is to discuss the method which will be used to predict the flow through such a postulated crack and present the leak rate calculation results for through-wall circumferential cracks.

5.2.1 General Considerations

The flow of hot pressurized water through an opening to a lower back pressure (causing choking) is taken into account. For long channels where the ratio of the channel length, L, to hydraulic diameter, D_H, (L/D_H) is greater than [--]^{a,c,e}, both [----------]^{a,c,e} must be considered. In this situation the flow can be described as being single-phase through the channel until the local pressure equals the saturation pressure of the fluid.

At this point, the flow begins to flash and choking occurs. Pressure losses due to momentum changes will dominate for [----------]^{a,c,e} However, for large L/D_H values, the friction pressure drop will become important and must be considered along with the momentum losses due to flashing.

5.2.2 Calculational Method

In using the [----------

----------]^{a,c,e}.

The flow rate through a crack was calculated in the following manner. Figure 5-2 from reference 5-2 was used to estimate the critical pressure, Pc, for the primary loop enthalpy condition and an assumed flow. Once Pc was found for a given mass flow, the [----------]^{a,c,e} was found from figure 5-3 taken from reference 5-2. For all cases considered, since [----------]^{a,c,e} Therefore, this method will yield the two-phase pressure drop due to momentum effects as illustrated in figure 5-4. Now using the assumed flow rate, G, the frictional pressure drop can be calculated using

$$\Delta P_f = [\quad]^{a,c,e} \qquad (5\text{-}3)$$

where the friction factor f is determined using the [----------]^{a,c,e} The crack relative roughness, ε, was obtained from fatigue crack data on stainless steel samples. The relative roughness value used in these calculations was [----------]^{a,c,e} RMS.

The frictional pressure drop using Equation 5-3 is then calculated for the assumed flow and added to the [----------
----------]^{a,c,e} to obtain the total pressure drop from the system under consideration to the atmosphere. Thus,

Absolute Pressure - 14.7 = [----------]^{a,c,e} (5-4)

for a given assumed flow G. If the right-hand side of equation 5-4 does not agree with the pressure difference between the piping under consideration and the atmosphere, then the procedure is repeated until equation 5-4 is satisfied to within an acceptable tolerance and this results in the flow value through the crack.

5.2.3 Leak Rate Calculations

Leak rate calculations were performed as a function of postulated through-wall crack length for the critical locations previously identified. The crack opening area was estimated using the method of reference 5-3 and the leak rates were calculated using the calculational methods described above. The leak rates were calculated using the normal operating loads at the governing node identified in section 4.0. The crack lengths yielding a leak rate of 10 gpm (10 times the leak detection capability of 1.0 gpm) for critical location at the Kewaunee Nuclear Plant pressurizer surge line are shown in Table 5-1.

The Kewaunee plant has an RCS pressure boundary leak detection system which is consistent with the guidelines of Regulatory Guide 1.45 for detecting leakage of 1 gpm in one hour.

5.3 Stability Evaluation

A typical segment of the pipe under maximum loads of axial force F and bending moment M is schematically illustrated as shown in figure 5-5. In order to calculate the critical flaw size, plots of the limit moment versus crack length are generated as shown in figures 5-6 to 5-13. The critical flaw size corresponds to the intersection of this curve and the maximum load line. The critical flaw size is calculated using the lower bound base metal tensile properties established in section 3.0.

The welds at the location of interest (i.e. the governing location) are SAW and SMAW. Therefore, "Z" factor correction for SMAW and SAW welds were applied (references 5-5 and 5-6) as follows:

$$Z = 1.15\ [1 + 0.013\ (O.D. - 4)]\ \text{(for SMAW)} \qquad (5\text{-}5)$$

$$Z = 1.30\ [1 + 0.010\ (O.D. - 4)]\ \text{(for SAW)} \qquad (5\text{-}6)$$

where OD is the outer diameter in inches. Substituting OD = 10.75 inches, the Z factor was calculated to be 1.25 for SMAW and 1.39 for SAW. The applied loads were increased by the Z factors and the plots of limit load versus crack length were generated as shown in figure 5-6 to 5-13. Table 5-2 shows the summary of critical flaw sizes for Kewaunee.

5.4 References

5-1 Kanninen, M. F. et al., "Mechanical Fracture Predictions for Sensitized Stainless Steel Piping with Circumferential Cracks" EPRI NP-192, September 1976.

5-2 [----------]a,c,e

5-3 Tada, H., "The Effects of Shell Corrections on Stress Intensity Factors and the Crack Opening Area of Circumferential and a Longitudinal Through-Crack in a Pipe," Section II-1, NUREG/CR-3464, September 1983.

5-4 NRC letter from M. A. Miller to Georgia Power Company, J. P. O'Reilly, dated September 9, 1987.

5-5 ASME Code Section XI, Winter 1985 Addendum, Article IWB-3640.

5-6 Standard Review Plan; Public Comment Solicited; 3.6.3 Leak-Before-Break Evaluation Procedures; Federal Register/Vol. 52, No. 167/Friday, August 28, 1987/Notices, pp. 32626-32633.

TABLE 5-1

Leakage Flaw Size

Node Point	Load Case	Temperature (°F)	Crack Length (in.) (for 10 gpm leakage)
1020	[		] a,c,e
.			
1240			

TABLE 5-2

Summary of Critical Flaw Size

Node Point	Load Case	Temperature (°F)	Critical Flaw Size (in)
1020	[		] a,c,e
1240			

a, c, e

Figure 5-1 Fully Plastic Stress Distribution

Figure 5-2 Analytical Predictions of Critical Flow Rates of Steam-Water Mixtures

Figure 5-3 [Critical or Choked]^{a,c,e} Pressure Ratio as a Function of L/D

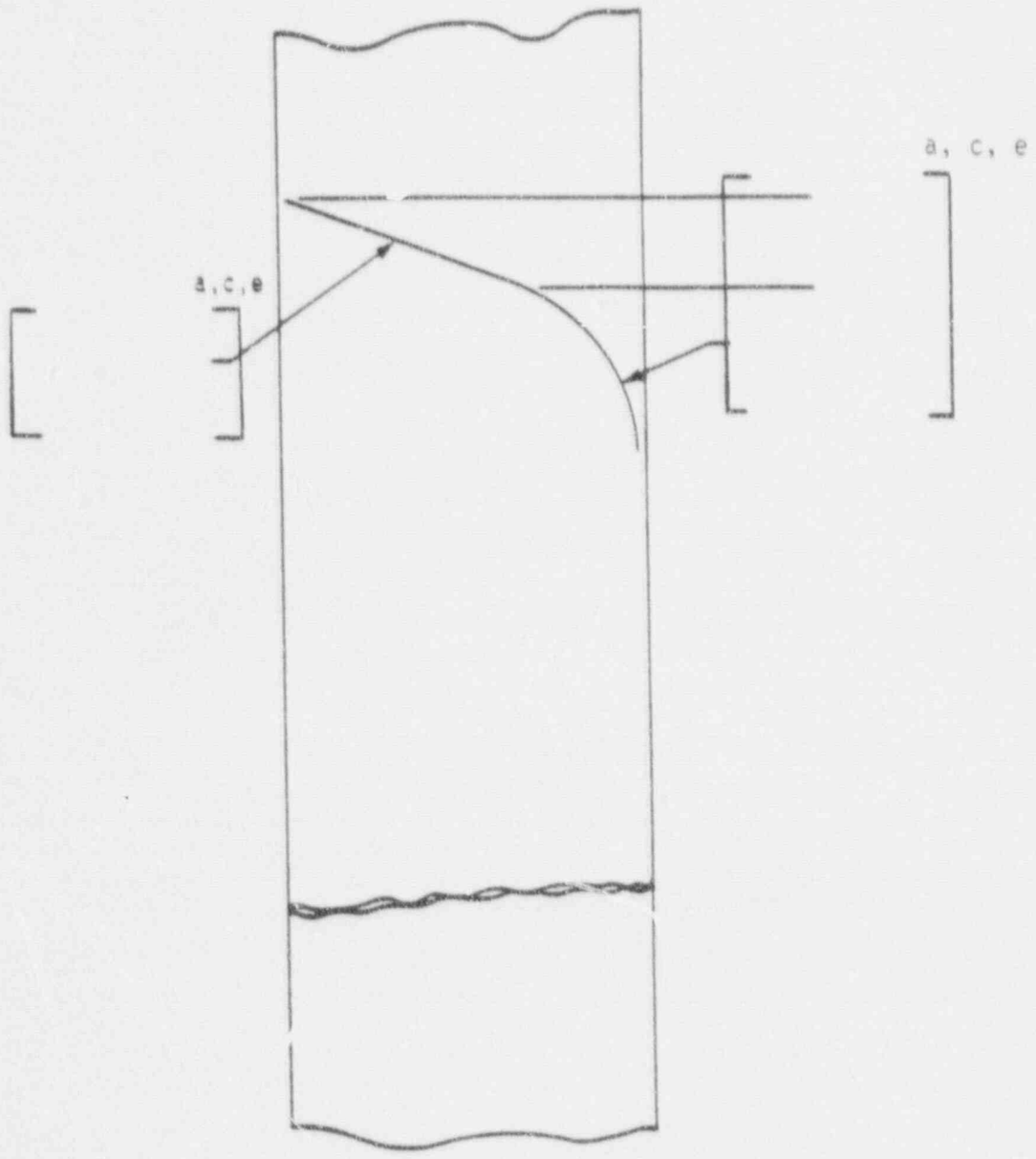

Figure 5-4. Idealized Pressure Drop Profile Through a Postulated Crack

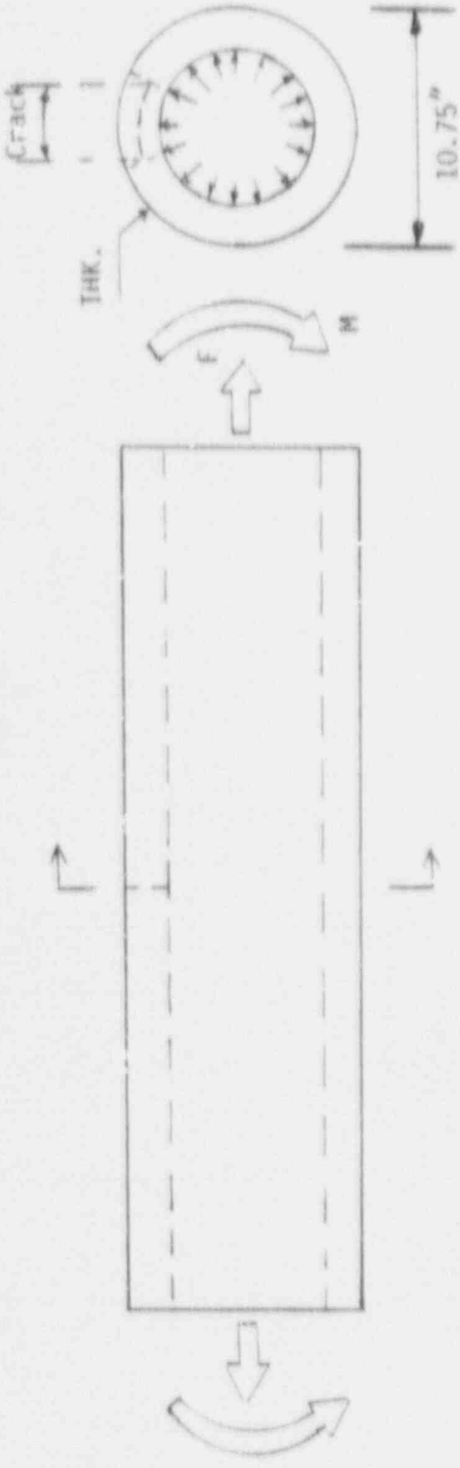

Figure 5-5. Loads Acting on the Model at the Governing Location

a, c, e

Figure 5-6. Critical Flaw Size Prediction for Node 1020 Case D

a, c, e

Figure 5-7. Critical Flaw Size Prediction for Node 1020 Case E

a, c, e

Figure 5-8 Critical Flaw Size Prediction for Node 1020 Case F

a, c, e

Figure 5-9 Critical Flaw Size Prediction for Node 1020 Case G

a, c, e

WPS CASE D NODE 1240(SAW)
PIPE OD=10.75 T= .880 SIGY=25.6 SIGU=77.9
Fa=150. M=.117E+04

Figure 5-10 Critical Flaw Size Prediction for Node 1240 Case D

a, c, e

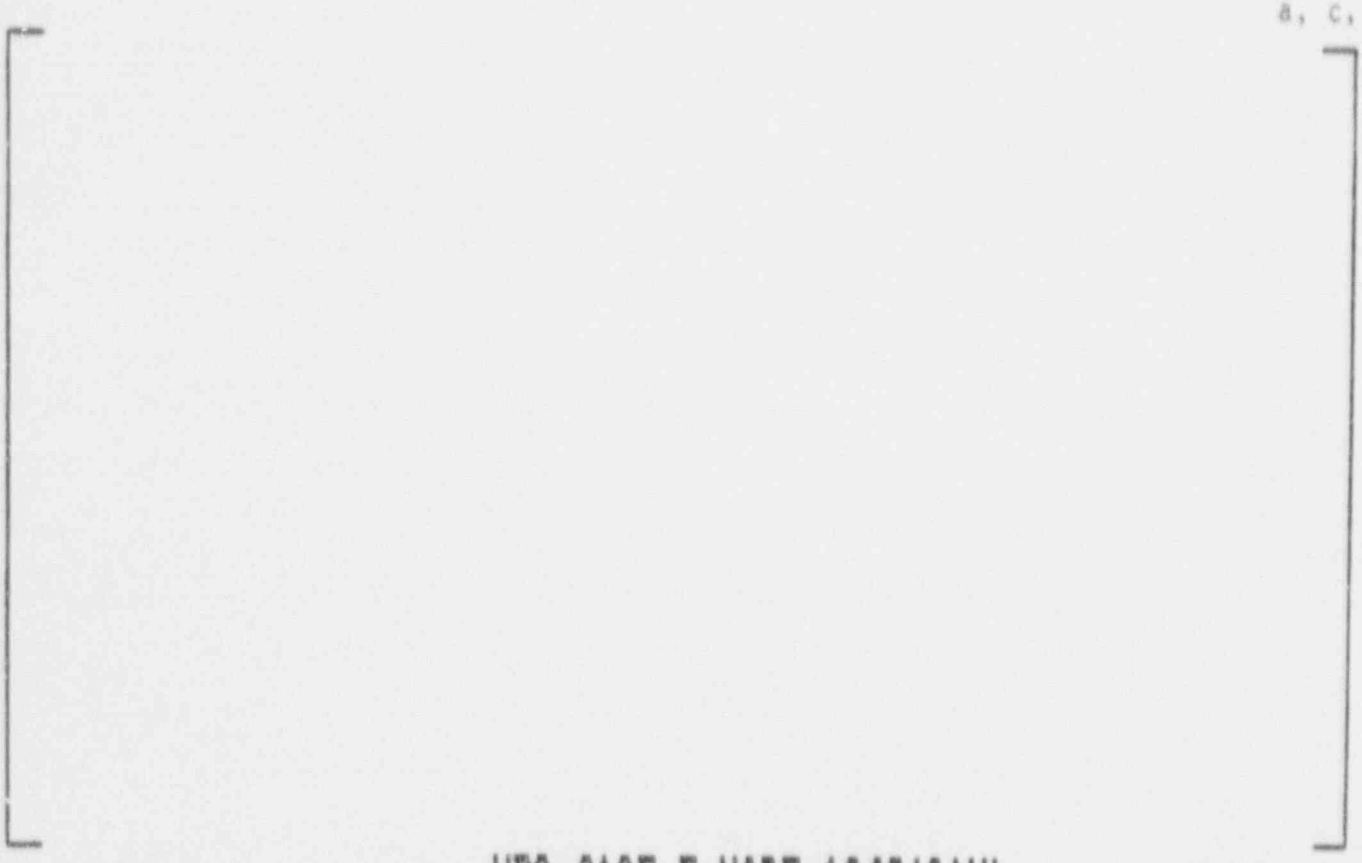

Figure 5-11 Critical Flaw Size Prediction for Node 1240 Case E

a, c, e

Figure 5-12 Critical Flaw Size Prediction for Node 1240 Case F

a, c, e

Figure 5-13 Critical Flaw Size Prediction for Node 1240 Case G

SECTION 6.0
ASSESSMENT OF FATIGUE CRACK GROWTH

6.1 Introduction

To determine the sensitivity of the pressurizer surge line to the presence of small cracks when subjected to the transients discussed in WCAP-12841, fatigue crack growth analyses were performed. This section summarizes the analyses and results.

Figure 6-1 presents a general flow diagram of the overall process. The methodology consists of seven basic steps as shown in figure 6-2. Steps 1 through 4 are discussed in WCAP-12841. Steps 5 through 7 are specific to fatigue crack growth and are discussed in this section.

There is presently no fatigue crack growth rate curve in the ASME Code for austenitic stainless steels in a water environment. However, a great deal of work has been done (References 6-1 and 6-2) which supports the development of such a curve. An extensive study was performed by the Materials Property Council Working Group on Reference Fatigue Crack Growth concerning the crack growth behavior of these steels in air environments, published in reference 6-1. A reference curve for stainless steels in air environments, based on this work, is in the 1989 Edition of Section XI of the ASME Code. This curve is shown in figure 6-3.

A compilation of data for austenitic stainless steels in a PWR water environment was made by Bamford (reference 6-2), and it was found that the effect of the environment on the crack growth rate was very small. For this reason it was estimated that the environmental factor should be set at 1.0 in the crack growth rate equation from reference 6-1. Based on these works (references 6-1 and 6-2) the fatigue crack growth law used in the analyses is as shown in figure 6-4.

6.2 Initial Flaw Size

Various initial surface flaws were assumed to exist. The flaws were assumed to be semi-elliptical with a six-to-one aspect ratio. The largest initial flaw assumed to exist was one with a depth equal to 10% of the nominal wall thickness, the maximum flaw size that could be found acceptable by Section XI of the ASME Code.

6.3 Results of FCG Analysis

Fatigue crack growth analyses were performed at locations 1 and 2 where detailed fracture; mechanics analyses as described in Sections 5 were completed. It should be noted that location 1 is near the reactor coolant loop nozzle and location 2 is near the pressurizer nozzle.

Results of the fatigue crack growth analysis are presented in table 6-1 for an initial flaw of 10% minimum wall thickness.

Conservatisms existing in the fatigue crack growth analysis are listed below.

1. Plant operational transient data has shown that the conventional design transients contain significant conservatisms.

[-- ----------

-- ----------

----------]^{a,c,e}

4. FCG neglects fatigue life prior to initiation.

6.4 References

6-1. James, L. A. and Jones, D. P., "Fatigue Crack Growth Correlations for Austenitic Stainless Steel in Air," in Predictive Capabilities in Environmentally Assisted Cracking, ASME publication PVP-99, December 1985.

6-2. Bamford, W. H., "Fatigue Crack Growth of Stainless Steel Reactor Coolant Piping in a Pressurized Water Reactor Environment," ASME Trans. Journal of Pressure Vessel Technology, Feb. 1979.

TABLE 6-1

FATIGUE CRACK GROWTH RESULTS FOR 10% OF WALL INITIAL FLAW SIZE

Location	Position	Initial Size (in)	Initial (% Wall)	Final (40 yr) Size (in)	Final Flaw (% Wall)
[					] a,c,e
-	-	-----	--	-----	-----
	-	-----	--	-----	-----
	-	-----	--	-----	-----
	-	-----	--	-----	----
-	-	-----	--	-----	----
	-	-----	--	-----	----
	-	-----	--	-----	----
	-	-----	--	-----	----

DETERMINATION OF THE EFFECTS OF THERMAL STRATIFICATION

a, c, e

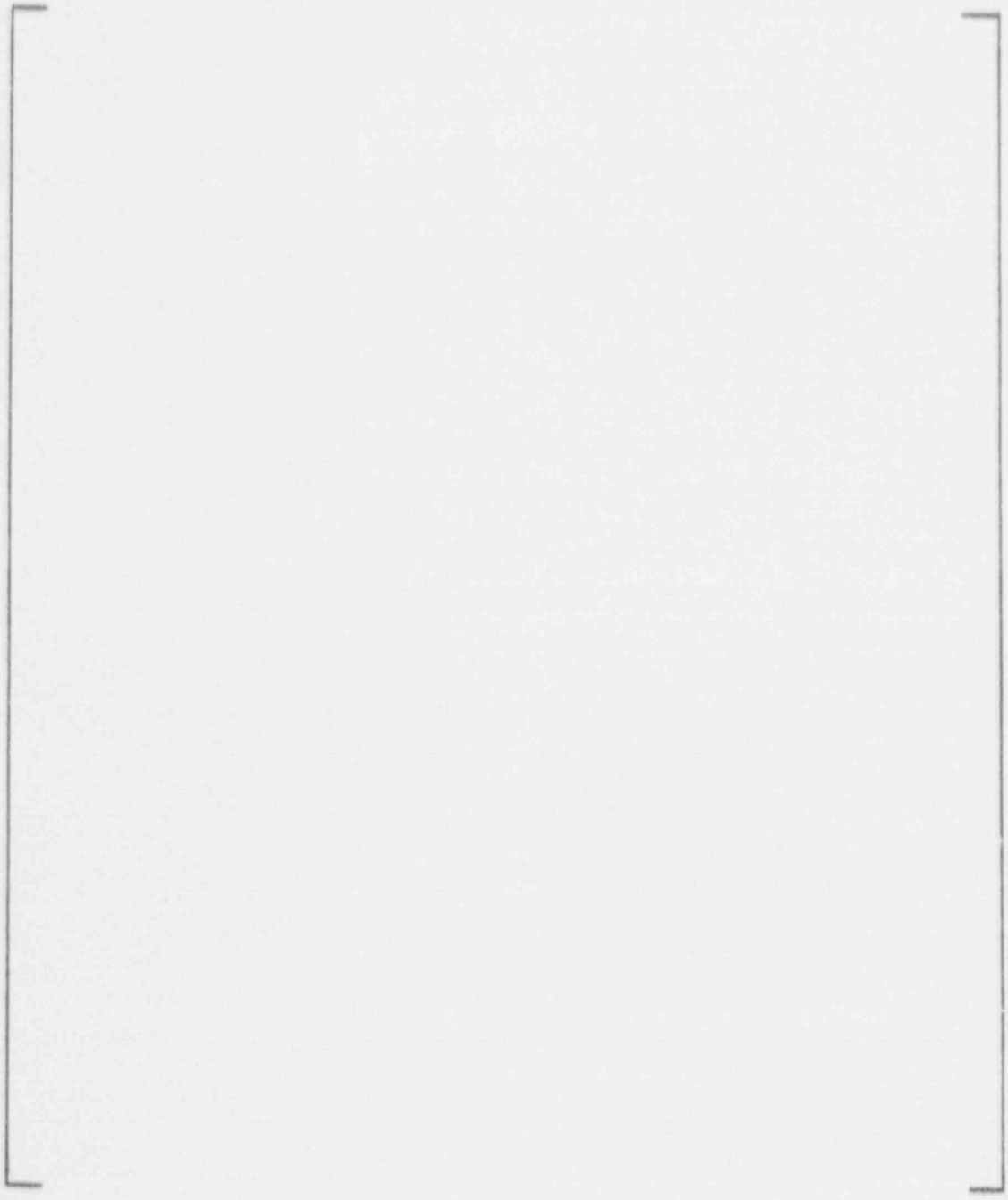

Figure 6-1 Determination of the Effects of Thermal Stratification on Fatigue Crack Growth

Figure 6-2 Fatigue Crack Growth Methodology

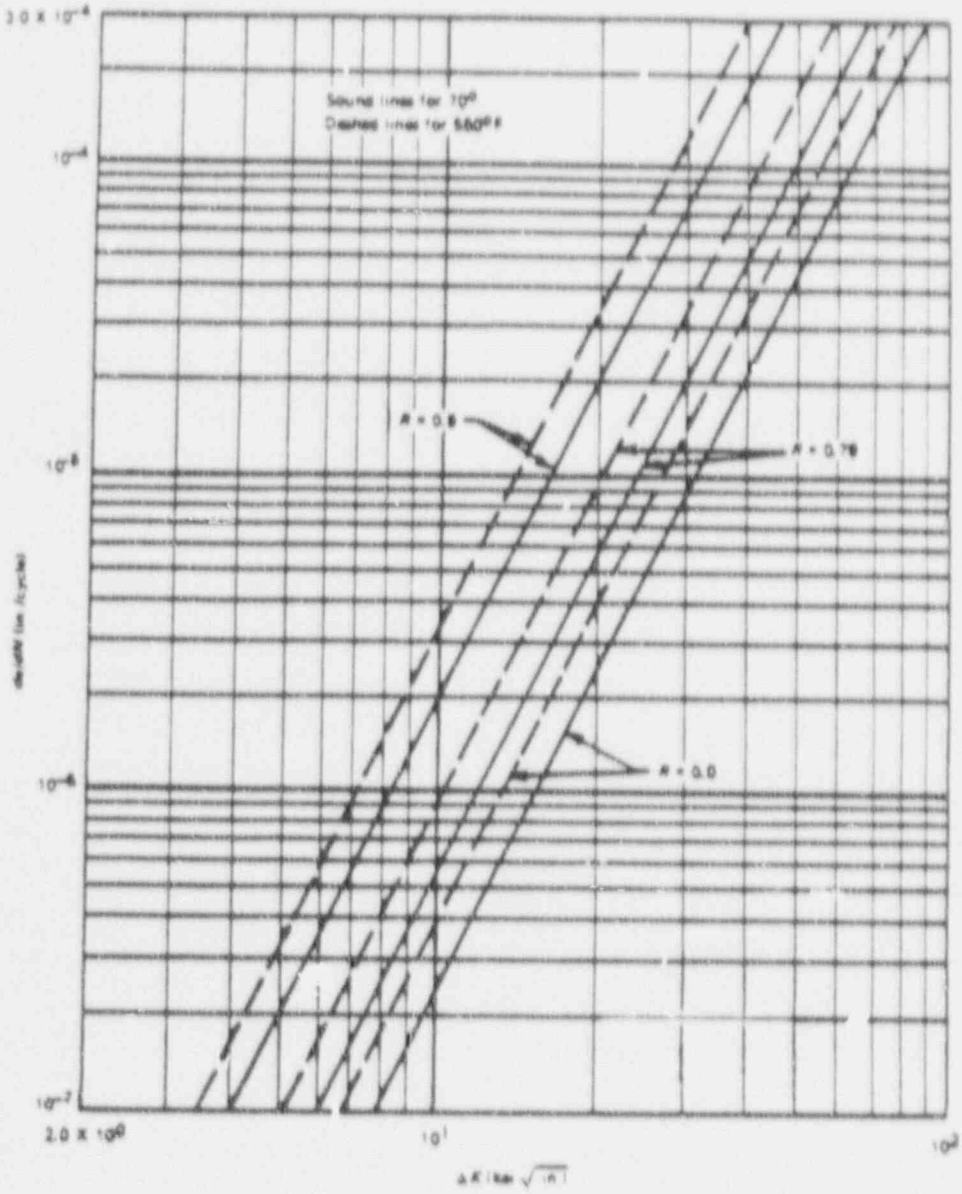

Figure 6-3 Fatigue Crack Growth Rate Curve for Austenitic Stainless Steel

$$\frac{da}{dn} = C\ F\ S\ E\ \Delta K^{3.30}$$

where

$\frac{da}{dn}$ = Crack Growth Rate in inches/cycle

C = 2.42×10^{-20}

F = Frequency factor (F = 1.0 for temperature below 800°F)

S = R ratio correction (S = 1.0 for R = 0; S = 1 + 1.3R for $0 < R < .8$; and S = -43.35 + 57.97R for $R > 0.8$)

E = Environmental Factor (E = 1.0 for PWR)

ΔK = Range of stress intensity factor, in psi $\sqrt{in}$

R = The ratio of the minimum K_I (K_{Imin}) to the maximum K_I (K_{Imax})

Figure 6-4. Fatigue Crack Growth Equation for Austenitic Stainless Steel

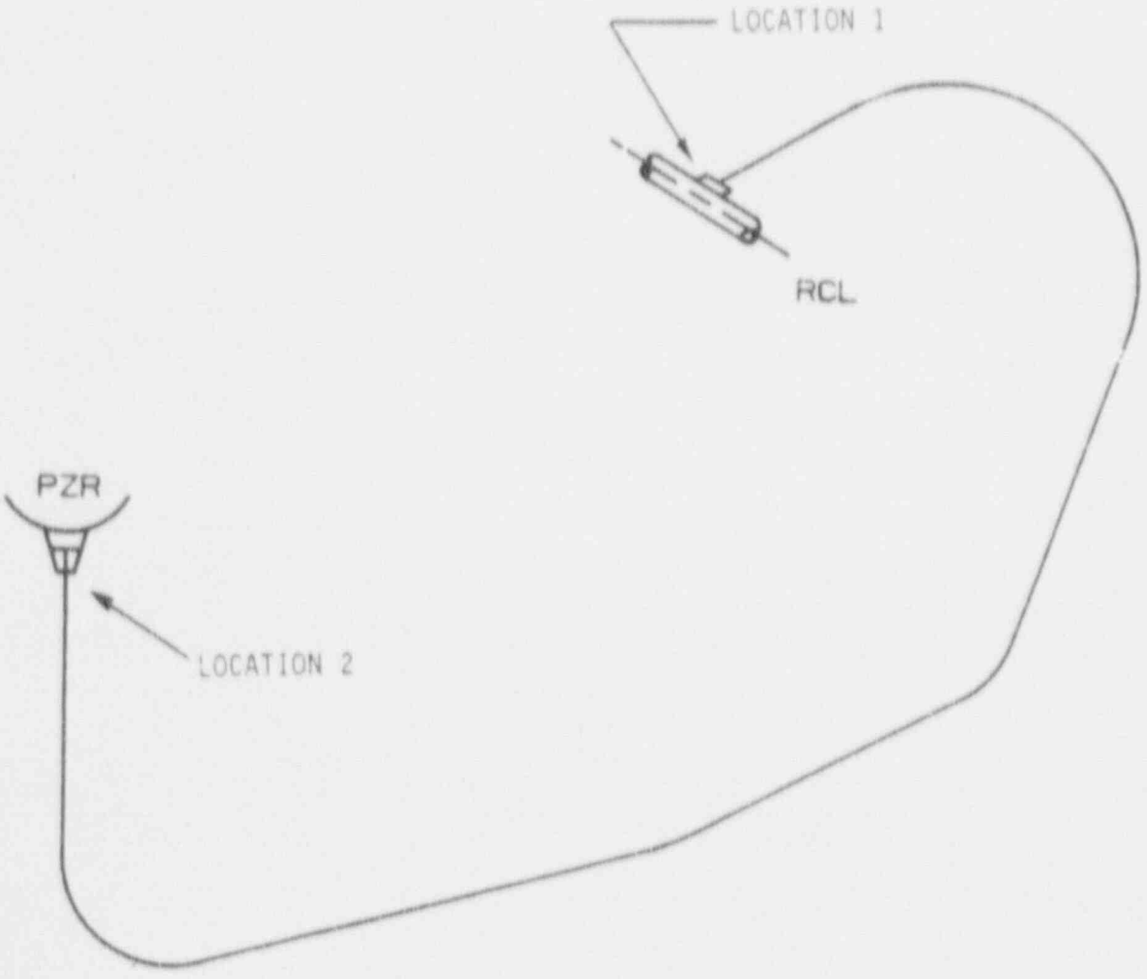

Figure 6-5. Fatigue Crack Growth Critical Locations

[ ] a,c,e

Figure 6-6. Fatigue Crack Growth Controlling Positions at Each Location

SECTION 7.0
ASSESSMENT OF MARGINS

In the preceding sections, the leak rate calculations, fracture mechanics analysis and fatigue crack growth assessment were performed. Margins at the critical location are summarized below:

In Secton 5.3 using the IWB-3640 approach (i.e. "Z" factor approach), the "critical" flaw sizes at the governing locations are calculated. In Section 5.2 the crack lengths yielding a leak rate of 10 gpm (10 times the leak detection capability of 1.0 gpm) for the critical locations are calculated. The leakage size flaws, the instability flaws, and margins are given in Table 7-1. The margins are the ratio of instability flaw to leakage flaw. The margins for analysis combination cases A/D, [----------]^{a,c,e} well exceed the factor of 2. The margin for the extremely low probability event defined by [--------]^{a,c,e} is [----------]^{a,c,e}. As stated in Section 4.3, the probability of simultaneous occurrence of SSE and maximum stratification due to shutdown because of leakage is estimated to be very low.

In this evaluation, the leak-before-break methodology is applied conservatively. The conservatisms used in the evaluation are summarized in Table 7-3.

TABLE 7-1

Leakage Flaw Sizes, Critical Flaw Sizes and Margins

Nozzle	[illegible]	Critical Flaw Size (in)	Leakage Flaw Size (in)	Margin	
1020	A/D	10.08	3.10	3.3	
	---	-----	----	---	a,c,e
	---	-----	----	---	
	---	-----	----	---	
	------	-----	----	---	
	------	-----	----	---	
1240	A/D	9.19	3.75	2.5	
	---	-----	----	---	a,c,e
	---	-----	----	---	
	---	-----	----	---	
	------	----	----	---	
	------	----	----	---	

[a] These are judged to be low probability events

TABLE 7-3

LBB Conservatisms

- Factor of 10 on Leak Rate
- Factor of 2 on Leakage Flaw for all cases (except for B/G which has 1.9 and it is a low probabilty case)
- Algabraic Sum of Loads for Leakage
- Absolute Sum of Loads for Stability
- Average Material Properties for Leakage
- Minimum Material Properties for Stability

SECTION 8.0
CONCLUSIONS

This report justifies the elimination of pressurizer surge line pipe breaks as the structural design basis for Kewaunee Nuclear Plant as follows:

a. Stress corrosion cracking is precluded by use of fracture resistant materials in the piping system and controls on reactor coolant chemistry, temperature, pressure, and flow during normal operation.

b. Water hammer should not occur in the RCS piping (primary loop and the attached class 1 auxiliary lines) because of system design, testing, and operational considerations.

c. The effects of low and high cycle fatigue on the integrity of the surge line were evaluated and shown acceptable. The effects of thermal stratification were evaluated and shown acceptable.

d. Ample margin exists between the leak rate of small stable flaws and the criterion of Reg. Guide 1.45.

e. Ample margin exists between the small stable flaw sizes of item d and the critical flaw size.

The postulated reference flaw will be stable because of the ample margins in d, e and will leak at a detectable rate which will assure a safe plant shutdown.

Based on the above, it is concluded that pressurizer surge line breaks should not be considered in the structural design basis of Kewaunee Nuclear Plant.

APPENDIX A

LIMIT MOMENT

APPENDIX A
LIMIT MOMENT

[

]a,c,e

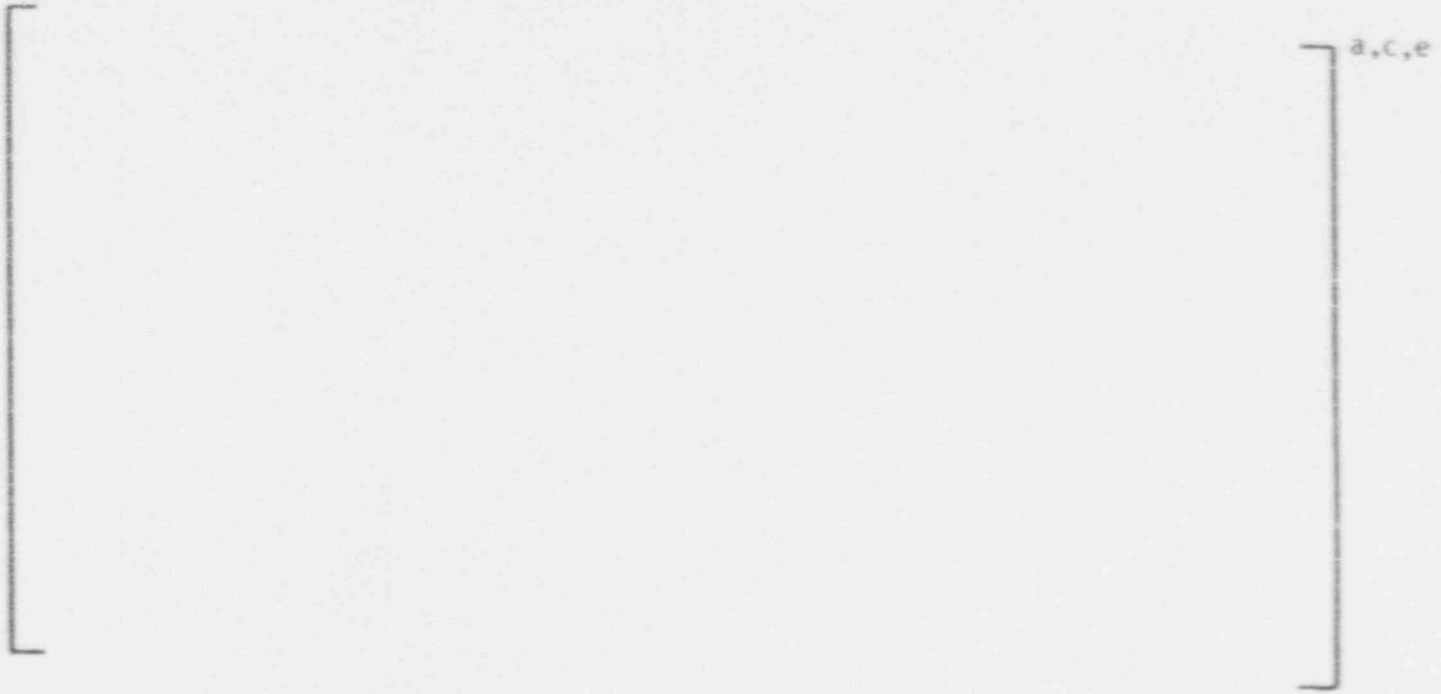

Figure A-1. Pipe With A Through-Wall Crack In Bending